



## Intercomparison of Sea Surface Salinity Products from SMOS, Aquarius and SMAP satellites

Emmanuel P. Dinnat<sup>(1,2)</sup>, David M. Le Vine<sup>(2)</sup>, Jacqueline Boutin<sup>(3)</sup>, Thomas Meissner<sup>(4)</sup>

(1) CEESMO, Chapman University, Orange, CA, U.S.A.

(2) NASA Goddard Space Flight Center, Greenbelt, MD, U.S.A.

(3) LOCEAN, Paris, France.

(4) Remote Sensing Systems, Santa Rosa, CA, U.S.A.

### Abstract

We present comparisons between satellite sea surface salinity products from the SMOS, Aquarius and SMAP missions and assess some of the reasons for the observed differences. We reprocess Aquarius retrievals using the dielectric constant model and ancillary sea surface temperature product used for SMOS. Then we quantify the impact of this on the differences between SMOS and Aquarius. We also validate the various Aquarius versions using in situ salinity measurements. Among the significant differences in retrieved sea surface salinity are the dependence on sea surface temperature and biases in coastal regions.

### 1. Introduction

Global fields of sea surface salinity estimates are available from three spaceborne L-band radiometer [1]–[3] for various periods over the last 7 years. Differences in instrument configuration and retrieval algorithm lead to differences in retrieved sea surface salinity (SSS). We report comparisons between SMOS, Aquarius and SMAP SSS products and comparisons with in situ observations from the Argo floats. The assessment reports large scale pattern, statistical distribution and temporal variation of the satellite retrieved SSS and in situ observations. We quantify the impact of some of the differences in retrieval algorithms on the SSS difference.

### 2. Data and methods

We use SMOS and SMAP level 3 SSS products which are Earth gridded at weekly or monthly time scales. For SMOS we use the product processed by the Laboratoire d'Océanographie et du Climat Expérimentations et Approches Numériques (LOCEAN). This product includes minimal empirical adjustment that allows us to explore the impact of retrieval parameters on the SSS errors. We use the Aquarius level 2 product which provides data along track at 1.44 sec resolution. We do not use the level 3 product in order to be able to reprocess the SSS retrieval using a modified algorithm to assess the impact of retrieval parameters. SMAP product is from Remote Sensing Systems. For the validation, we use in situ SSS from the Argo network of floats, which comprise about 4,000 floats performing a surface measurement

about every 10 days. For Argo, we define 'surface' as a depth of 10 m or less below the ocean surface. L-band radiometric measurements typically penetrate the first couple of centimeters of the ocean.

To assess the impact of the sea water dielectric constant and ancillary sea surface temperature (SST) product on the SSS retrievals and the differences between Aquarius/SMAP and SMOS, we reprocess the Aquarius retrievals using the Klein and Swift (KS) dielectric constant model [4] and the SST from the Operational Sea Surface Temperature and Sea Ice Analysis (OSTIA) system [5]. Both are used for SMOS processing. Aquarius uses the dielectric constant model by Meissner and Wentz [6] and the NOAA optimally interpolated daily SST [7].

All SSS products are re-gridded monthly at  $1^\circ \times 1^\circ$  resolution in latitude and longitude before the comparisons.

### 3. SSS comparisons

#### 3.1 Large scale patterns and statistical distribution

We compute difference maps between the three satellite products and the in situ observations from Argo (Figure 1). Differences between satellite SSS products, and between satellite and in situ SSS, exhibit strong latitudinal dependence, in part related to changes in SST. Other latitudinal differences have been linked to the eclipse seasons for the SMAP radiometer. We quantify the impact of SST, in terms of differences in the ancillary products or its impact on the dielectric constant in Section 4. Other notable differences between the SSS products include the varying impact of land contamination, with SMOS seeing the largest impact. SMAP and Aquarius land correction algorithm performs well in general, with a few notable exceptions such as the Mediterranean Sea being too fresh or the East and South coasts of Australia being too salty or fresh depending on the product.

The statistical distribution of SSS for the various products is broadly similar, with most SSS being between 33.8 and 35.8 psu, but there are some notable differences, particularly at the lower edge of the peak distribution in the range 33 - 33.8 psu. Some peaks in the Argo

histogram are missing from the satellite product or are present only in the Aquarius product. We will discuss the reasons for these discrepancies and the oceanic regions they are related to.

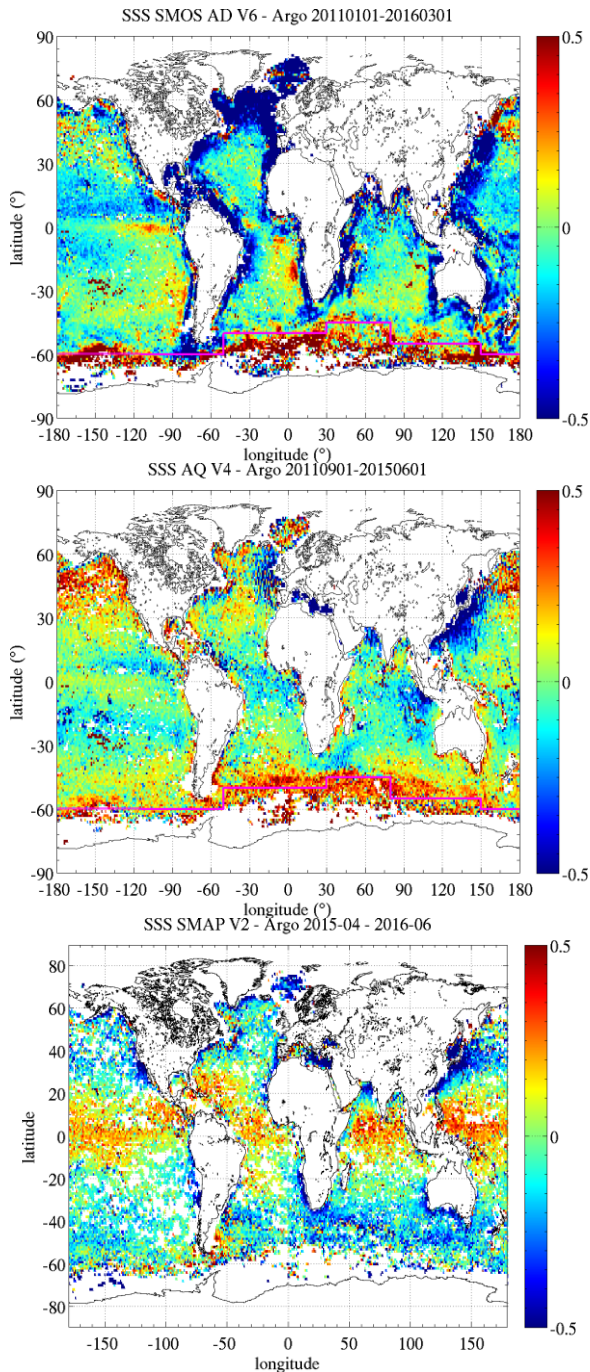


**Figure 1.** Map of difference between satellite SSS and in situ SSS from Argo for (a) SMOS, (b) Aquarius and (c) SMAP averaged over the period Sept 2011 – May 2015 for SMOS and Aquarius and April 2015 – June 2016 for SMAP.

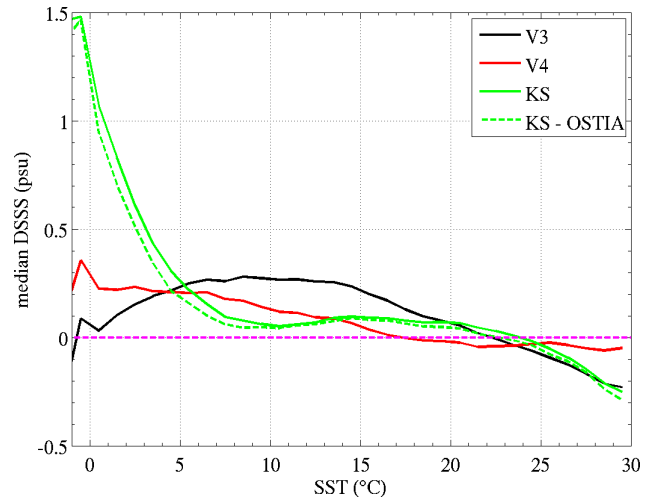


**Figure 2.** Median of the SSS difference between Aquarius retrievals and Argo observations as a function of SST for various retrieval algorithms. Differences are computed from 45 monthly SSS maps between Sept 2011 and May 2015. V3: version 3.0 of Aquarius SSS. V4: version 4.0 of Aquarius SSS which includes an empirical TB correction for the SST-dependent bias. KS: SSS retrieved from V3.0 TB and the KS dielectric constant model (instead of MW). KS-OSTIA: same as KS but using the OSTIA SST instead of NOAA OI.

### 3.2 Temporal variations

We assess the temporal variations of the SSS differences by defining 12 regions of interest (ROI) spread over various ocean basins and latitudes, covering various temperatures and SSS variability (e.g. close to the Amazon river outflow, at various ocean gyres, and in the equatorial Pacific Ocean). We quantify the SSS variations and biases with respect to Argo in the ROI for the various satellite products, including modified Aquarius product derived from changing the dielectric constant model and ancillary SST. We will discuss the performances of the various SSS products in tracking the seasonal and inter-annual variations in SSS.

### 4. Impact of ancillary SST and dielectric constant

We have reprocessed the Aquarius brightness temperatures (TB) to retrieve SSS using the same dielectric constant and ancillary SST as used for the SMOS retrieval. Differences in ancillary SST products have a relatively small influence on retrieved SSS ( $< 0.3$  psu) at low and mid latitudes because TB sensitivity to SST is small, except when the water is cold or warm. At high latitudes, SST differences can be large ( $> 2^{\circ}\text{C}$ ) and the increased sensitivity of TB to SST results in differences of 1 psu or more in SSS. Differences between SMOS and Aquarius SSS are reduced over the range  $6^{\circ}\text{C} - 20^{\circ}\text{C}$  when using the KS model for Aquarius retrievals. In order to assess if this also means an improvement in Aquarius SSS, we have compared Aquarius SSS using

different retrieval algorithm to Argo SSS (Figure 2). The match of Aquarius with Argo is best when using KS and OSTIA SST for SST between 6° and 20°C (excluding algorithm Version 4.0 which uses an empirical correction for the SST-dependent bias), but the error in Aquarius KS SSS becomes very large below 5°C.

## 5. Conclusion

We have compared SMOS, Aquarius and SMAP SSS products and related some of their differences to differences in the retrieval algorithm. We have evaluated various SSS retrieval algorithm with in situ SSS from Argo, in term of biases and temporal variations. The next version of the Aquarius product (V5) will use a new ancillary SST product and a modified atmospheric correction that impact the SSS dependence to SST. We will discuss how this changes the comparisons between satellites products and the validation with in situ SSS.

## 6. References

- [1] J. Font, A. Camps, A. Borges, M. Martin-Neira, J. Boutin, N. Reul, Y. H. Kerr, A. Hahne, and S. Mecklenburg, "SMOS: The challenging sea surface salinity measurement from space," *Proc. IEEE*, vol. 98, no. 5, pp. 649–665, 2010.
- [2] G. Lagerloef, F. R. Colomb, D. Le Vine, F. Wentz, S. Yueh, C. Ruf, J. Lilly, J. Gunn, Y. Chao, A. deCharon, G. Feldman, and C. Swift, "The Aquarius/SAC-D Mission: Designed to Meet the Salinity Remote-Sensing Challenge," *Oceanography*, vol. 21, no. 1, pp. 68–81, 2008.
- [3] D. M. Le Vine, E. P. Dinnat, T. Meissner, S. H. Yueh, F. J. Wentz, S. E. Torrusio, and G. Lagerloef, "Status of Aquarius/SAC-D and Aquarius Salinity Retrievals," *IEEE J. Sel. Top. Appl. Earth Obs. Remote Sens.*, vol. 8, no. 12, pp. 5401–5415, Dec. 2015.
- [4] L. A. Klein and C. T. Swift, "An improved model for the dielectric constant of sea water at microwave frequencies," vol. AP-25, no. 1, pp. 104–111, 1977.
- [5] C. J. Donlon, M. Martin, J. Stark, J. Roberts-Jones, E. Fiedler, and W. Wimmer, "The Operational Sea Surface Temperature and Sea Ice Analysis (OSTIA) system," *Remote Sens. Environ.*, vol. 116, pp. 140–158, 2012.
- [6] T. Meissner and F. J. Wentz, "The Emissivity of the Ocean Surface Between 6 and 90 GHz Over a Large Range of Wind Speeds and Earth Incidence Angles," vol. 50, no. 8, pp. 3004–3026, Aug. 2012.
- [7] R. W. Reynolds, T. M. Smith, C. Liu, D. B. Chelton, K. S. Casey, and M. G. Schlax, "Daily high-resolution-blended analyses for sea surface temperature," *J. Clim.*, vol. 20, no. 22, pp. 5473–5496, 2007.